Ana I. Pereira · Florbela P. Fernandes ·
João P. Coelho · João P. Teixeira ·
José Lima · Maria F. Pacheco ·
Luca Oneto · Rui P. Lopes (Eds.)

Communications in Computer and Information Science 2617

Optimization, Learning Algorithms and Applications

5th International Conference, OL2A 2025
Sesti Levante, Italy, April 28–30, 2025
Proceedings, Part I

Part 1

Springer

OL2A INTERNATIONAL CONFERENCE

Ana I. Pereira · Florbela P. Fernandes ·
João P. Coelho · João P. Teixeira · José Lima ·
Maria F. Pacheco · Luca Oneto · Rui P. Lopes
Editors

Optimization, Learning Algorithms and Applications

5th International Conference, OL2A 2025
Sesti Levante, Italy, April 28–30, 2025
Proceedings, Part I

Springer

Editors
Ana I. Pereira
Instituto Politécnico de Bragança
Bragança, Portugal

João P. Coelho
Instituto Politécnico de Bragança
Bragança, Portugal

José Lima
Instituto Politécnico de Bragança
Bragança, Portugal

Luca Oneto
University of Genoa
Genoa, Italy

Florbela P. Fernandes
Instituto Politécnico de Bragança
Bragança, Portugal

João P. Teixeira
Instituto Politécnico de Bragança
Bragança, Portugal

Maria F. Pacheco
Instituto Politécnico de Bragança
Bragança, Portugal

Rui P. Lopes
Instituto Politécnico de Bragança
Bragança, Portugal

ISSN 1865-0929 ISSN 1865-0937 (electronic)
Communications in Computer and Information Science
ISBN 978-3-032-00136-8 ISBN 978-3-032-00137-5 (eBook)
https://doi.org/10.1007/978-3-032-00137-5

This Springer imprint is published by the registered company Springer Nature Switzerland AG
The registered company address is: Gewerbestrasse 11, 6330 Cham, Switzerland

Preface

The volumes CCIS 2617 and 2618 contain the refereed proceedings of the V International Conference on Optimization, Learning Algorithms and Applications (OL2A 2025), a hybrid event held on April 28–30.

OL2A provided a space for the research community on optimization and learning to get together and share the latest developments, trends and techniques as well as develop new paths and collaborations. OL2A had the participation of more than two hundred participants in an online and face-to-face environment throughout three days, discussing topics associated with areas such as optimization and learning and state-of-the-art applications related to multi-objective optimization, optimization for machine learning, robotics, health informatics, data analysis, optimization and learning under uncertainty and the 4th industrial revolution.

Four special sessions were organized under the topics Artificial Intelligence in Healthcare and Medicine, Optimization in the SDG Context, Optimization in Control Systems Design, and Machine Learning and Artificial Intelligence in Robotics. The event had 38 accepted papers. All papers were carefully reviewed and selected from the 92 received submissions, with each paper receiving three double-blind reviews on average. All the reviews were carefully carried out by a scientific committee of 115 researchers from twenty-one countries.

April 2025

Ana I. Pereira
Florbela Fernandes
João P. Coelho
João P. Teixeira
José Lima
Maria F. Pacheco
Luca Oneto
Rui P. Lopes

Organization

General Chairs

Ana I. Pereira	Polytechnic Institute of Bragança, Portugal
Luca Oneto	University of Genoa, Italy

Program Committee Chairs

Florbela P. Fernandes	Polytechnic Institute of Bragança, Portugal
Maria de Fátima Pacheco	Polytechnic Institute of Bragança, Portugal
Rui Pedro Lopes	Polytechnic Institute of Bragança, Portugal
João P. Teixeira	Polytechnic Institute of Bragança, Portugal

Technology Chairs

João P. Coelho	Polytechnic Institute of Bragança, Portugal
José Lima	Polytechnic Institute of Bragança, Portugal

Program Committee

Ana Isabel Pereira	Polytechnic Institute of Bragança, Portugal
Abeer Alsadoon	Charles Sturt University, Australia
Ala' Khalifeh	German Jordanian University, Jordan
Alberto Nakano	Federal University of Technology – Paraná, Brazil
Alfonso González-Briones	University of Salamanca, Spain
Alexandre Douplik	Ryerson University, Canada
Ana Maria A. C. Rocha	University of Minho, Portugal
Ana Paula Teixeira	University of Trás-os-Montes and Alto Douro, Portugal
André Pinz Borges	Federal University of Technology – Paraná, Brazil
André Rodrigues da Cruz	Federal Center for Technological Education of Minas Gerais, Brazil
Andrej Košir	University of Ljubljana, Slovenia
Ângela Silva	University of Minho, Portugal
António José Sánchez-Salmerón	Universitat Politècnica de València, Spain

António Valente	University of Trás-os-Montes and Alto Douro, Portugal
Armando Mendes	University of the Azores, Portugal
Arnaldo Cândido Júnior	Federal Technological University – Paraná, Brazil
B. Rajesh Kanna	Vellore Institute of Technology, India
Bilal Ahmad	University of Warwick, UK
Bruno Bispo	Federal University of Santa Catarina, Brazil
C. Sweetlin Hemalatha	Vellore Institute of Technology, India
Carlos Henrique Alves	CEFET - Rio de Janeiro, Brazil
Carmen Galé	University of Zaragoza, Spain
Carolina Gil Marcelino	Federal University of Rio de Janeiro, Brazil
Christopher Expósito Izquierdo	University of La Laguna, Spain
Clara Vaz	Polytechnic Institute of Bragança, Portugal
Benjamín J. González Díaz	University of La Laguna, Spain
Damir Vrančić	Jožef Stefan Institute, Slovenia
Dhiah Abou-Tair	German Jordanian University, Jordan
Diamantino Silva Freitas	University of Porto, Portugal
Diego Brandão	CEFET - Rio de Janeiro, Brazil
Dimitris Glotsos	University of West Attica, Greece
Eduardo Vinicius Kuhn	Federal Technological University – Paraná, Brazil
Elaine Mosconi	Université de Sherbrooke, Canada
Eligius M. T. Hendrix	University of Málaga, Spain
Felipe Nascimento Martins	Hanze University of Applied Sciences, Netherlands
Florbela P. Fernandes	Polytechnic Institute of Bragança, Portugal
Florentino Fernández Riverola	University of Vigo, Spain
Francisco Sedano	University of León, Spain
Fredrik Danielsson	University West, Sweden
Gaukhar Muratova	Dulaty University, Kazakhstan
Gediminas Daukšys	Kauno Technikos Kolegija, Lithuania
Gianluigi Ferrari	University of Parma, Italy
Glaucia Maria Bressan	Federal University of Technology – Paraná, Brazil
Glotsos Dimitris	University of West Attica, Greece
Helena Sofia Rodrigues	Polytechnic Institute of Viana do Castelo, Portugal
Humberto Rocha	University of Coimbra, Portugal
Heba M. Afify	Cairo University, Egypt
Ismael Delgado	University of Málaga, Spain
João Paulo Carmo	University of São Paulo, Brazil
João Paulo Coelho	Polytechnic Institute of Bragança, Portugal
João Paulo Teixeira	Polytechnic Institute of Bragança, Portugal
Jorge Igual	Universitat Politècnica de València, Spain

Jorge Garcia	Polytechnic Institute of Viana do Castelo, Portugal
Jorge Ribeiro	Polytechnic Institute of Viana do Castelo, Portugal
José Boaventura-Cunha	University of Trás-os-Montes and Alto Douro, Portugal
José Cascalho	University of the Azores, Portugal
José Lima	Polytechnic Institute of Bragança, Portugal
Joseane Pontes	Federal University of Technology – Ponta Grossa, Brazil
Josip Musić	University of Split, Croatia
Juan A. Méndez Pérez	University of La Laguna, Spain
Juan Alberto García Esteban	University of Salamanca, Spain
Júlio Cesar Nievola	Pontifícia Universidade Católica do Paraná, Brazil
Kristina Sutiene	Kaunas University of Technology, Lithuania
Laura Belli	University of Parma, Italy
Lidia Sánchez	University of León, Spain
Lino Costa	University of Minho, Portugal
Luca Davoli	University of Parma, Italy
Luca Oneto	University of Genoa, Italy
Luca Spalazzi	Marche Polytechnic University, Italy
Luis Antonio De Santa-Eulalia	Université de Sherbrooke, Canada
Luís Coelho	Polytecnhic Institute of Porto, Portugal
Maria de Fátima Pacheco	Polytechnic Institute of Bragança, Portugal
Mahmood Reza Khabbazi	University West, Sweden
Manuel Castejón Limas	University of León, Spain
Marc Jungers	Université de Lorraine, France
Marco Aurélio Wehrmeister	Federal University of Technology – Paraná, Brazil
Marek Nowakowski	Military Institute of Armoured and Automotive Technology, Poland
Maria do Rosário de Pinho	University of Porto, Portugal
Martin Hering-Bertram	Hochschule Bremen, Germany
Mattias Bennulf	University West, Sweden
Michał Podpora	Opole University of Technology, Poland
Miguel Ángel Prada	University of León, Spain
Mikulas Huba	Slovak University of Technology in Bratislava, Slovakia
Milena Pinto	Federal Center of Technological Education Celso Suckow da Fonseca, Brazil
Miroslav Kulich	Czech Technical University in Prague, Czech Republic
Nicolae Cleju	Technical University of Iasi, Romania
Paulo Alves	Polytechnic Institute of Bragança, Portugal

Paulo Lopes dos Santos	University of Porto, Portugal
Paulo Medeiros	University of the Azores, Portugal
Paulo Moura Oliveira	University of Trás-os-Montes and Alto Douro, Portugal
Pavel Pakshin	Nizhny Novgorod State Technical University, Russia
Pedro Luiz de Paula Filho	Federal Technological University – Paraná, Brazil
Pedro Morais	Polytechnic Institute of Cávado e Ave, Portugal
Pedro Pinto	Polytechnic Institute of Viana do Castelo, Portugal
Roberto Molina de Souza	Federal University of Technology – Paraná, Brazil
Rui Pedro Lopes	Polytechnic Institute of Bragança, Portugal
Sabrina Šuman	Polytechnic of Rijeka, Croatia
Sancho Salcedo Sanz	University of Alcalá, Spain
Sandro Dias	Federal Center for Technological Education of Minas Gerais, Brazil
Santiago Torres Álvarez	University of La Laguna, Spain
Sara Paiva	Polytechnic Institute of Viana do Castelo, Portugal
Shridhar Devamane	Global Academy of Technology, India
Sławomir Stępień	Poznań University of Technology, Poland
Sudha Ramasamy	University West, Sweden
Teresa Paula Perdicoulis	University of Trás-os-Montes and Alto Douro, Portugal
Toma Rancevic	University of Split, Croatia
Virginia Castillo	University of León, Spain
Vítor Duarte dos Santos	Nova University Lisbon, Portugal
Vitor Pinto	University of Porto, Portugal
Vivian Cremer Kalempa	State University of Santa Catarina, Brazil
Wojciech Giernacki	Poznań University of Technology, Poland
Wojciech Paszke	University of Zielona Gora, Poland
Wynand Alkema	Hanze University of Applied Sciences, Netherlands
Zahia Guessoum	University of Reims Champagne-Ardenne, France

Deep Learning

A Deep Learning Approach for Average Height Estimation in Oak Colony Using RGB Images

Raphael Duarte Britto[1,2(✉)], João Mendes[1(✉)], Vinicius Grilo[1(✉)], João P. Castro[3(✉)], Murillo Ferreira dos Santos[2(✉)], Marina Castro[3(✉)], Ana I. Pereira[1(✉)], and José Lima[1(✉)]

[1] CeDRI, SusTEC, Instituto Politécnico de Bragança, Campus de Santa Apolónia, 5300-253 Bragança, Portugal
{raphael,joao.cmendes,viniciusgrilo,jllima,apereira}@ipb.pt

[2] Centro Federal de Educação Tecnológica de Minas Gerais (CEFET-MG), Minas Gerais 36700-000, Brazil
murillo.ferreira@cefetmg.br

[3] CIMO, SusTEC, Instituto Politécnico de Bragança, Campus de Santa Apolónia, 5300-253 Bragança, Portugal
jpmc@ipb.pt

Abstract. Many strategies have been developed to monitor the volume of volume of Above Ground Biomass (AGB) in forest areas as a fundamental step for managing carbon concentration. This study explores the use of use of Light Detection and Ranging (LiDAR) data obtained through Unmanned Aerial Vehicles (UAVs) to estimate height values in a vegetation colony composed of oaks (*Quercus pyrenaica* Willd.) in northern Portugal. The extraction of pertinent information from LiDAR data was facilitated by using the LAStools extension within the Quantum Geographic Information System (QGIS) software framework. The generated raster and image information were used to calculate the height values of the vegetation. Following this extraction, the information was meticulously organized into datasets, which were then employed in Deep Learning (DL) algorithms. The VGG16 model was selected as the underlying framework for the present study. Height predictions were made using dimensions of 16×16, 32×32, and 64×64 pixels for the Red, Green and Blue (RGB) images. The data was estimated and compared using both the standard format of the VGG16 model and a superficially adapted version of its convolution layers. The algorithm's efficacy was validated by comparing the forecast results with the data obtained from QGIS, which revealed minimal discrepancies. It was observed that using 64×64 pixel scale images yielded enhanced accuracy, resulting in reduced values for the Mean Absolute Error (MAE). The study demonstrates the viability of applying DL techniques to accurately capture information about a forest area using RGB images.

Keywords: Deep Learning · LiDAR · QGIS · RGB Images · VGG16

A. I. Pereira et al. (Eds.): OL2A 2025, CCIS 2617, pp. 272–285, 2026.
https://doi.org/10.1007/978-3-032-00137-5_19

1 Introduction

Human activity is one of the main causes of climate change and global warming [23]. The emission of gases that contribute to the worsening of the greenhouse effect, such as carbon dioxide, can be attributed to burning fossil fuels, deforestation, and intensified urban sprawl [17]. One of the solutions to mitigate the proportions of such occupations can be seen in the development of ecological plans, such as European Green Deal (EGD). The political strategy aims to monitor and regulate the carbon emissions applied to each country belonging to the European Union, promoting a short transition to a sustainable economy [11]. Therefore, sustainable agricultural practices such as regenerative agriculture and the preservation of plant regions are encouraged by EGD, with the aim of normalizing emission rates.

The needs for uninterrupted observation of plant areas has resulted in the employment of technological resources [13]. Among these resources, satellites are an advantageous option in terms of cost-benefit ratio, allowing one to obtain information by taking images over large areas. However, due to their low spatial resolution and cloud cover, this device often becomes inconsistent when seeking a more precise extraction of information. To overcome this data inconsistency, using Unmanned Aerial Vehicle (UAV) is becoming increasingly promising for collecting data with greater precision, considering scans of small areas. With more refined precision, it is possible to use a UAV to carry out a more specific study of a vegetation area, as is the case for surveying a forest inventory [16]. The precise analysis of a forest inventory can result in valuable information, such as the volume of Above Ground Biomass (AGB) and, consequently, the amount of carbon concentrated in the region.

To estimate the AGB in a plant population, it is important that its dendrometric data, such as total height and Diameter at Breast Height (DBH), are accurately extracted. The variety of information provided using sensor Light Detection and Ranging (LiDAR) data makes this tool ideal for estimating AGB from forest inventories. UAV-based LiDAR technology offers high versatility regarding flight paths and information collection [9]. It is possible to obtain a more accurate point cloud as the scanner gets closer to the reflection points [18]. Although an ideal option, this technology can be limited by the forest's density and the region's topography. It is, therefore, recommended that a scan be made above the canopy and briefly manipulated to obtain satisfactory results.

The high vertical accuracy of LiDAR allows the scan information to be stored as Digital Elevation Models (DEMs), providing a point cloud with the elevation value for each pixel. The main vegetation height analysis procedure is subtracting Digital Terrain Model (DTM) from Digital Surface Model (DSM). In this way, obtaining the vegetation height values at each point is possible, ignoring the topographic elevation. In addition, each point is stored with Red, Green and Blue (RGB) information, making it possible to display the point cloud in raster format [9]. However, the canopy cover in the scan area can make data collection difficult. There are some alternatives to get around this challenge, such as categorizing, filtering, and interpolating a point cloud [16]. The software Quantum Geographic

Information System (QGIS) is an ideal tool when working with point clouds containing georeferenced information [15]. The LAStools extension offers various options for processing LiDAR data, making it possible to analyze information represented by point clouds.

After processing LiDAR data, the diversity of information stored makes it possible to estimate the height of plant regions and sub-regions before resulting in an AGB value in the same location [14]. The use of Convolutional Neural Networks (CNNs), specifically DL algorithms, has been increasingly initiated in the field of science and technology [4]. With numerous advantages, such as high learning capacity and adaptation to data distribution, the application of DL is essential when seeking to estimate AGB through LiDAR data [28]. The study region's real data, collected in situ, was presented to evaluate the results obtained by DL [3].

However, this study aims to estimate the average total height of a plant colony, which is essential information for conducting a forest inventory. The data was collected using a UAV-based LiDAR and briefly processed using the LAStools extension of the QGIS software. With the information extracted from the LiDAR data, vegetation heights were estimated with DL algorithms using RGB images. Following the training phase of the algorithm, it is anticipated that RGB images obtained by means other than LiDAR, such as camera images, will become a viable option. Based on the analysis of the prediction results, a plan for future work and adaptations is presented, showing possible improvements and dissemination of the approach.

The study presented in this paper is divided into six sections. Section 2 describes the study region and the methodology and analysis of the data obtained; Sect. 3 presents the results of the data analysis; Sect. 4 develops a detailed analysis of the results obtained and identifies opportunities for future studies; Sect. 5 presents the conclusion of the results; and Sect. 6 highlights points for improvement and future steps in this study.

2 Materials and Methods

This section presents the stages and methods used in this study. First, the research area is presented, detailing each data format analyzed and their respective datasets. The section describes the algorithmic model used and the analysis metrics used to examine the results.

2.1 Study Environment

The study was carried out in the locality of Zeive $41°5'29.5''N$ $6°53'39.4''W$, a region belonging to the municipality of Bragança, in northeastern Portugal. The region's climate is classified as Csb (temperate with dry and mild summers), with an altitude of about $900m$ above sea level [2]. The study area covers about $35000m^2$, with vegetation consisting mainly of oak trees, especially *Quercus pyrenaica* [10]. Being a deciduous species, it shows significant variation in its

concentration and leaf color throughout the seasons, with a marked decrease in the fall. Furthermore, the specie demonstrates optimal growth during the spring and summer seasons [27]. However, these seasons are slightly delayed in consideration of the region's altitude [20]. Consequently, in Zeive, the species' effective growing season is approximated from June to October.

2.2 Field Data

Four sub-regions were delimited to extract dendrometric data from the vegetation, arbitrarily named CB1, CB2, CAc1, and CAc2 (Fig. 1). Each plot covers an area of about $800m^2$, and the forest inventory data was collected using the Draudt method [19]. As such, plant information was not recorded in its entirety. All trees' data relating to DBH was recorded, while trees classified as dominant or sample had their information recorded in full. DBHs measurements were obtained using a $50cm$ Haglöf Sweden probe. Height measurements were collected using a Vertéx IV [8] hypsometer. All information was collected in January 2024.

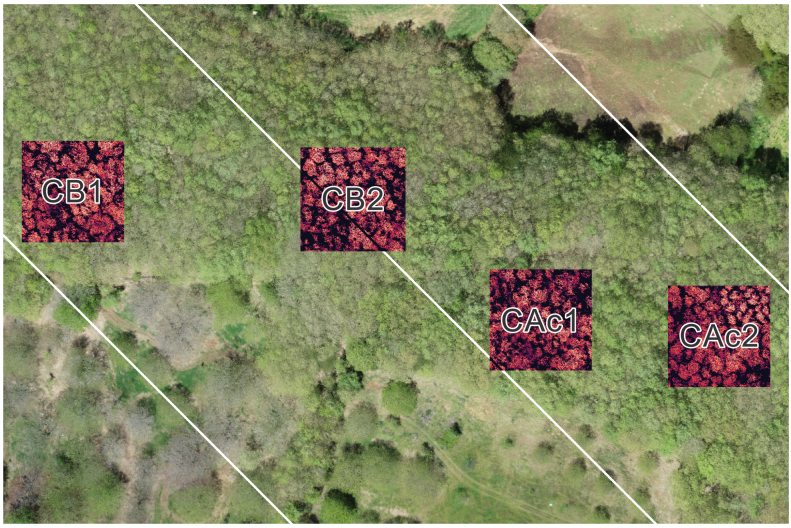

Fig. 1. Highlighting the four study sub-regions and their approximate boundaries in the RGB raster displayed by the QGIS software.

It is important to note that despite the lack of demarcated data for common trees (not classified as dominant or sample), the necessary information was obtained for subsequent application in hypsometric equations. Their total height values were estimated based on specific coefficients for the species [26]. The hypsometric equation presented in Equation (1) was used.

$$h = \frac{d}{\beta_0 + \beta_1 d}, \tag{1}$$

where h is the total height, d the DBH, β_0 the coefficient of 0.8073, and β_1 of 0.0573 for oaks [25].

Then, the average total heights were calculated for each sub-region using actual (dominant trees or sample) and estimated total height data. The values for each sub-region are shown in Table 1, as well as the global average and standard deviation (SD).

Table 1. Average total height values obtained between measured and estimated data for the total height of trees in each sub-region

Sub-Region	Average Total Height (m)	Global Average (m)	SD (m)
CB1	11.0035	10.8141	0.1442
CB2	10.7357		
CAc1	10.6742		
CAc2	10.8429		

In the course of this study, the mean values were accompanied by the calculation of the standard deviation, thus demonstrating the variability within a given set of values. Following the calculation, it was established that 95% of the samples used for the calculation did not deviate significantly from the SD value [1]. The formula for calculating the SD is given in Equation (2):

$$SD = \sqrt{\frac{\sum_{i=1}^{n} (\overline{x} - x_i)^2}{n-1}}, \tag{2}$$

where i is the value index, n is the number of samples, $\overline{x}$ is the average of the sample values, and x_i is the sample value referenced by the index [12].

2.3 LiDAR Data Processing by QGIS

The region was scanned using the Zenmuse L1 LiDAR sensor [6] carried by a DJI Matrice 300 RTK UAV (Fig. 2) [5]. Global navigation satellite system real-time kinematic (GNSS RTK) technology gives the Matrice 300 RTK centimeter-level accuracy to the ground during flight. Inertial measurement units (IMUs) are also used to provide accurate direct georeferencing of the aircraft [7]. The flight plan was created using DJI Pilot v2.5.1.10 software in May 2024, after which the data was applied to DJI Terra v4.0.10 to generate the point cloud in .las format. Once the data had been collected, QGIS v3.34.11 processed the LiDAR data.

LiDAR data is stored in the ".las" format, which consists of a georeferenced point cloud. Extracting this format allows the analysis of individual information, such as Tagged Image File Formats (TIFFs) data, which, in this case, defines the

Fig. 2. The UAV-based LiDAR set employed to collect LiDAR data from the study site.

vertical distances (elevation) of each pixel obtained by scanning. To process the LiDARs data, tools provided by the LAStools extension to the QGIS software were used. DEMs were generated to obtain the forest height in the region. To do this, the elevation information was filtered through the first lidar return, forming the study area's Digital Terrain Model (DTM), as shown in Fig. 3a. Subsequently, the last return was used as a filter to obtain the Digital Surface Model (DSM) shown in Fig. 3b. Subtraction of the two layers produced a Height Model (CHM), which contains the vegetation height in each scan pixel. For a brief treatment of the data, a reclassification of the data was carried out, removing the negative data present in the CHM (Fig. 3c).

Similarly, in this case, the TIFF format displays height information, while the RGB data displays the color of each pixel stored by the LiDAR. When displayed as a raster, the set of RGB information can resemble an image (Fig. 3d) and can be treated as such. Given the four sub-regions (CB1, CB2, CAc1, and CAc2) delineated for field data collection, the same extensions were delineated in the RGB representation of this study, as shown in Fig. 1. The process was aided by georeferencing the LiDAR data. The images in RGB were then divided into 16×16, 32×32, and 64×64 pixel dimensions using Python. Furthermore, a larger data set was created, which favors the use of RGB images as input data for DL algorithms.

Splitting the RGB images of each sub-region resulted in a larger volume of data, which favored the subsequent use of the split images as input data for DL algorithms. However, the RGB color scale images require a value to relate them to the search variable, in this case, vegetation height. To do this, we used the information from the TIFF file in each pixel provided by the previously generated CHM raster. For each RGB image, an average height value was assigned based on the elevation values of each pixel within the extent of the image itself. It is important to note that during data manipulation in the QGIS software, some

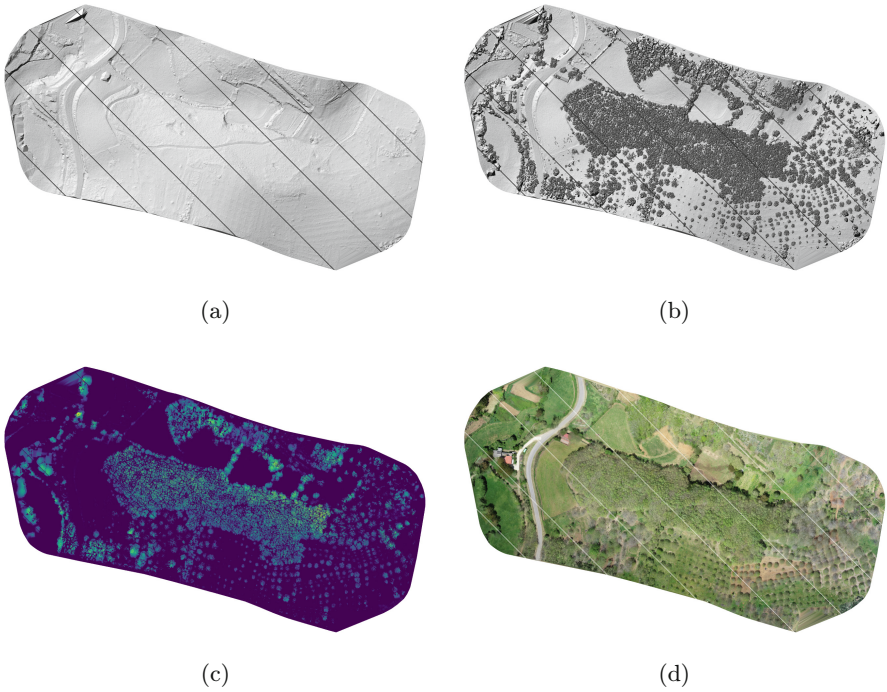

Fig. 3. Extraction of TIFF and RGB information in the QGIS software using the tools provided by the LAStools extension: (a) DTM; (b) DSM; (c) reclassified CHM; (d) raster RGB.

watermarks overlapped some extensions of the study sub-regions. As a solution, all images with imperfections were removed from the dataset, 48 images in total.

Finally, the useful data were saved as ".csv" files, represented by a "filename" column, which identifies the divided RGB image, and a second "height" column, which refers to the average between the TIFF values of the pixels delimited by their respective image. A total of fifteen datasets were obtained. The number of labels stored in each dataset is shown in Table 2.

Table 2. Number of labels in each dataset

Dataset	CB1	CB2	CAc1	CAc2	Mixed	Total
16×16	289	279	286	289	1143	1453
32×32	64	59	63	64	250	
64×64	16	13	15	16	60	

The elevation data obtained from LiDAR scans and processed in QGIS software provides a detailed estimate of the average elevation of the terrain. How-

ever, a significant discrepancy was observed when these values were validated with data collected directly in the field. For the same area, the manual measurements indicated average heights of around 10 m, while the data derived from LiDAR showed significantly lower average values of around 5 m.

Analysing into the possible causes of this discrepancy revealed that the lowest values, below 1 m, disproportionately influenced calculating the average height. These values, which often represent undergrowth or shrubs, are methodologically different from field measurements, which only include large trees and ignore shrubs. The discrepancy between the data collection approaches compromised the direct comparability between the two data sets.

To mitigate this problem and to prepare the data to the methodology used in the field, a filter was implemented that ignored (assigned null values, NaN) all observations with heights below $1.3m$. The height of $1.3m$ is justified as a minimum threshold for characterizing large trees in forest or agricultural areas [21]. The value of $1.3m$ is widely used in dendrometric studies and corresponds to the standard height for measuring DBH, a metric often adopted for forest inventories analysis [24]. This criterion reflects the exclusion of undergrowth and shrubs and brings the LiDAR data into line with the range of manual field measurements.

After applying the filter, the average height values derived from the LiDAR data were much closer to the field measurements. The discrepancy between the values was significantly reduced, increasing the reliability of the LiDAR data for training the deep learning model. As shown in Table 3, this adjustment resulted in a significant improvement in the average heights read by the LiDAR (considering the four sub-regions for each pixel dimension) and the average calculated in the field.

Table 3. Comparison of values obtained from LiDAR data processed in QGIS (without filtering and validating only values above $1.3m$) with field data

Dataset		Average Total Height (m)		SD (m)
QGIS	16×16	5.2074	5.1038 (no filtering)	0.1409
	32×32	5.1607		
	64×64	4.9433		
	16×16	7.8503	7.8859 (above 1.3 filtering)	0.0652
	32×32	7.9611		
	64×64	7.8463		
Field Data	CB1	11.0035	10.8351 (Draudt method)	0.1442
	CB2	10.7357		
	CAc1	10.6742		
	CAc2	10.9268		

The filtering stage was crucial in ensuring that the data used in the study more accurately reflected the real characteristics of the area in question, providing a solid basis for estimating heights using a DL model. Furthermore, this approach highlights the need to consider methodological differences when integrating data sources in scientific studies.

2.4 Deep Learning Models Configuration

To estimate tree heights from RGB images (organized into labels, Table 2) captured by UAV, we chose to use a DL model based on Convolutional Neural Networks (CNNs). CNNs are a class of neural networks specifically designed for image analysis that exploit the spatial hierarchy of visual data to extract relevant features. These models have demonstrated high performance in computer vision tasks due to their ability to learn complex spatial patterns automatically.

Among the several models available, we choose VGG16, an architecture introduced by Simonyan and Zisserman in 2014 as part of the ImageNet Large Scale Visual Recognition Challenge (ILSVRC) competition [22]. VGG16 consists of 16 trainable layers organized in convolution blocks, followed by pooling and fully connected layers. Its main advantage lies in its structural simplicity, with small convolutional filters (3×3), which makes it efficient in extracting features without compromising the depth of the model [22]. Furthermore, its widespread use in the literature and its proven robustness make it a suitable choice for computer vision applications.

However, due to the limitations imposed by the minimum size of images processed by this network (typically 224×224 pixels), it was necessary to modify the architecture to work with 16×16 pixel images while retaining the essence of the VGG16 convolutional approach.

To enable the analysis of 16×16 pixel images, a reduced version of VGG16 was developed. The modified model retains the basic structure of convolution and pooling but presents a reduction in the number of layers to adapt to the limitations imposed by the size of the image. The modified version of the model can be seen in Fig. 4.

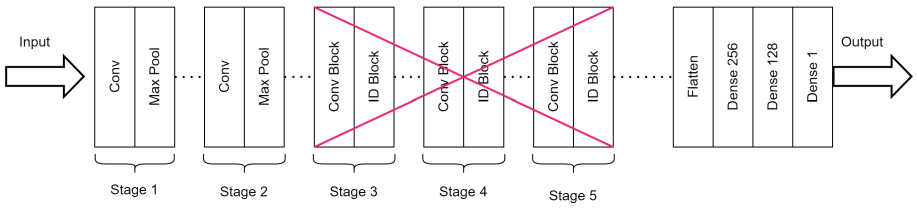

Fig. 4. Architecture of the modified VGG16 model, adapted for 16×16 pixel images. The structure retains the core convolutional and pooling layers, with fewer layers accommodating the lower image resolution.

The model starts with convolutional layers that extract features, followed by dense layers that perform regression. In contrast to the original version of VGG16, it was necessary to reduce the convolutional layers and simplify the architecture to cope with the lower resolution of the images. ReLU activation was used in all hidden layers to ensure non-linearity and better gradient propagation. The Adam algorithm optimized the model due to its convergence efficiency and stability in minimizing the loss function, which is Mean Square Error (MSE).

MAE metric was used as an additional reference to assess the quality of the predictions, providing a more intuitive interpretation of the average error between the estimated heights and the QGIS values organized into labels. The formula for calculating the MAE is given in Eq. 3:

$$MAE = \frac{1}{n} \sum_{j=1}^{n} |y_j - \widehat{y}_j| \,, \tag{3}$$

where j is the sample index, y_j is the observed value referenced by the index, and $\widehat{y}_j$ is the estimated value.

This metric makes monitoring and analyzing the algorithm's performance easier. The trained model was then evaluated on the test set to verify its generalization ability. The results are discussed in the next section.

3 Results

The average results recorded by QGIS and estimated by DL and MAE for each dataset are shown in Table 4.

Table 4. Average results obtained by applying the VGG16 model, both in standard and modified format, as well as the average QGIS and MAE values obtained for each dataset

Model	Image Dimension (px)	QGIS (m)	Deep Learning (m)	MAE
VGG16 (modified)	16×16	7.8503	7.8113	1.3592
	32×32	7.9611	7.9183	1.1619
	64×64	7.8463	7.9986	0.9364
VGG16 (standard)	32×32	7.9611	7.6683	1.0469
	64×64	7.8463	8.0469	0.7938

It can be seen that the MAE values are lower for datasets with larger RGB images. The best results were obtained using the VGG16 model in its default configuration, specifically considering using RBG images with dimensions of 64×64 pixels, resulting in an average MAE value of 0.7938. The worst result, 1.3592, was recorded using 16×16 pixel RGB images in the adapted VGG16 model. This suggests that the accuracy of a dataset is proportional to the size of its images.

In parallel, the standard model of the VGG16 algorithm showed better results compared to the adapted model. The standard format showed values of 1.0469 and 0.7938, while the adapted model reached values of 1.1619 and 0.9364 for 32×32 and 64×64 pixel images, respectively. Thus, the standard VGG16 algorithm provides greater accuracy for the estimated data, especially when using 64×64 pixel RGB images.

4 Discussion

It should be noted that the UAV scans were carried out during the period of dense canopy and, since this is a deciduous species (*Quercus pyrenaica* Willd.), the season of the year directly interferes with the visuals obtained from the RGB images extracted from the LiDAR data. This scenario delineates a set of variables as a potential source of interference in the performance of the trained algorithm, given that the input data are RGB images. However, it is advisable to repeat the procedure for a season characterized by leaf fall and color change, which was not considered in this first study.

An evaluation threshold has been applied, taking into account only the points recorded above $1.3m$ (using the DBH parameter), in order to reduce the discrepancy between the height averages obtained by DL and those measured in the field. In any case, there is a need for a parameterization that relates the total height data from the field to the average height data from the DL forecast.

The use of images in RGB format, with proportions of 64×64 pixels, resulted in lower values of MAE, with values of 0.9364 and 0.7938 for the adapted and standard formats of the VGG16 algorithm, respectively. These results suggest that the results obtained from 64×64 pixel images are more reliable than the others. The algorithm generally accurately estimated the average total height from reduced dimension RGB images based on heights extracted from lidar data. This can be seen by analyzing that the global average for MAE values is around 1.0, indicating a deviation of about 1 m for the average total height.

For experimental purposes, applying the algorithm to 1×1 pixel dimensions of RGB images was briefly analyzed and did not produce favorable results. This result can be explained by the fact that the model did not identify patterns between the features presented by the images in question. Therefore, the study of images with a single-pixel aspect ratio was not included in the data validation stages and was only carried out to learn about the model used.

5 Conclusion

This study presents an approach for estimating the average total height in a forest colony using RGB images. In fact, several studies related to forest repository consider the use of technologies that facilitate the procedure, such as the use of UAVs and LiDAR data, which are widely discussed and well regarded in this scenario. Each procedure already developed has its own peculiarities, whether in terms of the methods adopted, their complexity, or their similarity. The tactic

described in this paper represents a simplified but efficient solution for obtaining average height values in a forest colony.

The data processed for analysis was obtained by scanning with a UAV-based LiDAR over the height of the canopy. QGIS software was used to process and extract relevant information from the LiDAR data, extracting image and height information, which was then organized into labels. It is important to note that field data recorded on the same plot was also analyzed for a quick comparison of the manipulated data. An insignificant discrepancy with the field data was observed when all TIFF information was considered to determine average heights. Thus, only TIFF values greater than 1.3 were validated, reducing the initial difference between the field data and QGIS. After the appropriate manipulation, fifteen datasets containing an average height value for each RGB image of the study site were generated.

After processing, the data was sent to the VGG16 algorithm to make predictions of average total heights. As the 16×16 pixel image size would not be compatible with VGG16's native configuration, its convolutional layers were slightly modified. The results were thus obtained in two stages: (a) using the adapted VGG16 model for three image dimensions (16×16, 32×32, and 64×64) and (b) using the algorithm's standard format for 32×32 and 64×64 pixel images. To analyze the data estimated by DL, based on the information extracted by the QGIS software, the MAE metric was applied. In its generalization, the research obtained results of considerable precision, showing discrepancies of about 1 m between the QGIS data and those estimated by DL. The best result was obtained using 64×64 pixel images in the standard VGG16 format, achieving 0.7938 for MAE. The worst result was obtained when processing 16×16 pixel images using the adapted format, reaching 1.3592. Despite the convergence between QGIS values and those estimated by DL, both showed a slight deviation when compared to real values measured in the field.

6 Future Works

The work was carried out on a limited set of variables to obtain an initial validation. By reducing the margins of error and complexity, this restriction certainly favors the satisfactory accuracy obtained. The results estimated by DL showed great consistency compared to the values obtained in QGIS from LiDAR data. However, they showed a significant difference when compared directly with the values obtained on the ground. This is a promising avenue that merits further exploration to advance the study.

This initial study raises the possibility of applying the described procedure in different circumstances. A more comprehensive method, considering different factors, is expected to be evaluated for different tree species, seasons, and possibly algorithmic models. With a more complete and parameterized model, it will be possible to develop weightings for estimating the volume of AGB. This will provide more concrete guidance on the feasibility of applying the method to carbon prediction using RGB images, the ultimate motivation for developing this work.

Acknowledgments. This study was funded by iCarbono project Fundação La Caixa (PL23-00038) and LIFE SILFORE project (LIFE21-CCA-ES-LIFE). The authors are also grateful to CeDRI (UID/05757), SusTEC (LA/P/0007/2021), CIMO (UIDP/00690/2020), CEFET-MG and the National Council for Scientific and Technological Development – CNPq, related to project 442696/2023-0.

Disclosure of Interests. The authors have no competing interests to declare relevant to this article's content.

References

1. Altman, D.G., Bland, J.M.: Standard deviations and standard errors. BMJ **331**(7521), 903 (2005)
2. Instituto Português do Mar e da Atmosfera (IPMA): IPMA - Clima Normais (2025). https://www.ipma.pt/opencms/en/oclima/normais.clima/1971-2000/
3. Chen, L., Ren, C., Zhang, B., Wang, Z., Xi, Y.: Estimation of forest above-ground biomass by geographically weighted regression and machine learning with sentinel imagery. Forests **9**(10), 582 (2018)
4. Dalla Corte, A.P., et al.: Forest inventory with high-density UAV-lidar: machine learning approaches for predicting individual tree attributes. Comput. Electron. Agricult. **179**, 105815 (2020)
5. DJI: Matrice 300 RTK Product Sheet (2020). https://www.dji.com/matrice-300/downloads
6. DJI: Zenmuse L1 Product Sheet (2021). https://www.dji.com/zenmuse-l1/downloads
7. Eker, R., Alkan, E., Aydın, A.: A comparative analysis of UAV-RTK and UAV-PPK methods in mapping different surface types. Euro. J. Forest Eng. **7**(1), 12–25 (2021)
8. Haglöf Sweden AB: Vertex IV product sheet, technical specification document for the Vertex IV ultrasound hypsometer. Includes Details on Features, Specifications, and Usage in Forestry Applications (2016)
9. Harkel, J., Bartholomeus, H., Kooistra, L.: Biomass and crop height estimation of different crops using UAV-based lidar. Remote Sens. **12**(1), 17 (2019)
10. Jardim Botânico UTAD: Ficha técnica quercus pyrenaica (nd), informações compiladas pela equipa do Jardim Botânico UTAD. A utilização está regida pelos termos e condições gerais de utilização da Flora Digital de Portugal. http://jb.utad.pt
11. Johnson, C., et al.: The bio-based industries joint undertaking as a catalyst for a green transition in Europe under the European green deal. EFB Bioecon. J. **1**, 100014 (2021)
12. Lee, D.K., In, J., Lee, S.: Standard deviation and standard error of the mean. Korean J. Anesthesiol. **68**(3), 220–223 (2015)
13. Lee, G., Wei, Q., Zhu, Y.: Emerging wearable sensors for plant health monitoring. Adv. Func. Mater. **31**(52), 2106475 (2021)
14. Li, W., Niu, Z., Chen, H., Li, D., Wu, M., Zhao, W.: Remote estimation of canopy height and aboveground biomass of maize using high-resolution stereo images from a low-cost unmanned aerial vehicle system. Ecol. Ind. **67**, 637–648 (2016)
15. Maesano, M., Santopuoli, G., Moresi, F.V., Matteucci, G., Lasserre, B., Scarascia Mugnozza, G.: Above ground biomass estimation from UAV high resolution RGB images and lidar data in a pine forest in southern Italy. iForest-Biogeosci. Forestry **15**(6), 451 (2022)

16. Mao, P., et al.: An improved approach to estimate above-ground volume and biomass of desert shrub communities based on UAV RGB images. Ecol. Ind. **125**, 107494 (2021)
17. Matiza, C., Mutanga, O., Peerbhay, K., Odindi, J., Lottering, R.: Assessing above-ground biomass in reforested urban landscapes using machine learning and remotely sensed data. J. Spatial Sci., 1–28 (2024)
18. Neuville, R., Bates, J.S., Jonard, F.: Estimating forest structure from UAV-mounted lidar point cloud using machine learning. Remote Sens. **13**(3), 352 (2021)
19. Patrício, M.S., Dias, C.R., Nunes, L.: Mixed-effects generalized height-diameter model: a tool for forestry management of young sweet chestnut stands. For. Ecol. Manage. **514**, 120209 (2022)
20. Ranjitkar, S.: Effect of elevation and latitude on spring phenology of Rhododendron at Kanchenjunga conservation area, East Nepal. Int. J. Appl. Sci. Biotechnol. **1**(4), 253–257 (2013)
21. Saatchi, S.S., et al.: Benchmark map of forest carbon stocks in tropical regions across three continents. Proc. Natl. Acad. Sci. **108**(24), 9899–9904 (2011)
22. Simonyan, K., Zisserman, A.: Very deep convolutional networks for large-scale image recognition. arXiv preprint arXiv:1409.1556 (2015)
23. Solomon, S., Plattner, G.K., Knutti, R., Friedlingstein, P.: Irreversible climate change due to carbon dioxide emissions. Proc. Natl. Acad. Sci. **106**(6), 1704–1709 (2009)
24. Sumida, A., Miyaura, T., Torii, H.: Relationships of tree height and diameter at breast height revisited: analyses of stem growth using 20-year data of an even-aged *Chamaecyparis obtusa* stand. Tree Physiol. **33**(1), 106–118 (2013)
25. Tomé, M., Meyer, A., Ramos, T., Barreiro, S., Faias, S., Cortiçada, A.: Relações hipsométricas e equações de diâmetro da copa desenvolvidas no âmbito do tratamento dos dados do inventário florestal nacional 2005–2006. Publicações GIMREF. RT **3**, 2007 (2007)
26. Tomé, M., Barreiro, S., Paulo, J.A., Faias, S.P.: Selecção de equações para estimação de variáveis da árvore em inventários florestais a realizar em portugal. Publicações FORCHANGE PT **9** (2007)
27. Vasconcellos, J.D.C., Franco, J.D.A.: Carvalhos de portugal. Anais do Instituto Superior de Agronomia, vol. 21 (1954)
28. Zhang, L., Heuvelink, G.B., Mulder, V.L., Chen, S., Deng, X., Yang, L.: Using process-oriented model output to enhance machine learning-based soil organic carbon prediction in space and time. Sci. Total Environ. **922**, 170778 (2024)